Cross Section and Parity-Violating Spin Asymmetries of $W^{\pm}$ Boson Production in Polarized $p + p$ Collisions at $\sqrt{s} = 500$ GeV

A. Adare,[11] S. Afanasiev,[25] C. Aidala,[34] N. N. Ajitanand,[56] Y. Akiba,[50,51] R. Akimoto,[10] J. Alexander,[56] H. Al-Ta'ani,[44] K. R. Andrews,[1] A. Angerami,[12] K. Aoki,[50] N. Apadula,[57] E. Appelt,[61] Y. Aramaki,[10] R. Armendariz,[6] E. C. Aschenauer,[5] T. C. Awes,[46] B. Azmoun,[5] V. Babintsev,[21] M. Bai,[4] B. Bannier,[57] K. N. Barish,[6] B. Bassalleck,[43] A. T. Basye,[1] S. Bathe,[51] V. Baublis,[49] C. Baumann,[39] A. Bazilevsky,[5] R. Belmont,[61] J. Ben-Benjamin,[40] R. Bennett,[57] A. Berdnikov,[53] Y. Berdnikov,[53] D. S. Blau,[30] J. S. Bok,[63] K. Boyle,[51] M. L. Brooks,[34] D. Broxmeyer,[40] H. Buesching,[5] V. Bumazhnov,[21] G. Bunce,[5,51] S. Butsyk,[34] S. Campbell,[57] A. Caringi,[40] P. Castera,[57] C.-H. Chen,[57] C. Y. Chi,[12] M. Chiu,[5] I. J. Choi,[22,63] J. B. Choi,[8] R. K. Choudhury,[3] P. Christiansen,[36] T. Chujo,[60] O. Chvala,[6] V. Cianciolo,[46] Z. Citron,[57] B. A. Cole,[12] Z. Conesa del Valle,[32] M. Connors,[57] M. Csanád,[15] T. Csörgő,[28] S. Dairaku,[31,50] A. Datta,[38] G. David,[5] M. K. Dayananda,[18] A. Denisov,[21] A. Deshpande,[51,57] E. J. Desmond,[5] K. V. Dharmawardane,[44] O. Dietzsch,[54] A. Dion,[24] M. Donadelli,[54] L. D'Orazio,[37] O. Drapier,[32] A. Drees,[57] K. A. Drees,[4] J. M. Durham,[57] A. Durum,[21] Y. V. Efremenko,[46] T. Engelmore,[12] A. Enokizono,[46] H. En'yo,[50,51] S. Esumi,[60] B. Fadem,[40] D. E. Fields,[43] M. Finger, Jr.,[7] M. Finger,[7] F. Fleuret,[32] S. L. Fokin,[30] J. E. Frantz,[45] A. Franz,[5] A. D. Frawley,[17] Y. Fukao,[50] T. Fusayasu,[42] I. Garishvili,[58] A. Glenn,[33] X. Gong,[56] M. Gonin,[32] Y. Goto,[50,51] R. Granier de Cassagnac,[32] N. Grau,[12] S. V. Greene,[61] M. Grosse Perdekamp,[22] T. Gunji,[10] L. Guo,[34] H.-Å. Gustafsson,[36,*] J. S. Haggerty,[5] K. I. Hahn,[16] H. Hamagaki,[10] J. Hamblen,[58] J. Hanks,[12] R. Han,[48] C. Harper,[40] K. Hashimoto,[52,50] E. Haslum,[36] R. Hayano,[10] T. K. Hemmick,[57] T. Hester,[6] X. He,[18] J. C. Hill,[24] R. S. Hollis,[6] W. Holzmann,[12] K. Homma,[20] B. Hong,[29] T. Horaguchi,[60] Y. Hori,[10] D. Hornback,[46] S. Huang,[61] T. Ichihara,[50,51] R. Ichimiya,[50] H. Iinuma,[27] Y. Ikeda,[50,52,60] K. Imai,[31,50] M. Inaba,[60] A. Iordanova,[6] D. Isenhower,[1] M. Ishihara,[50] M. Issah,[61] A. Isupov,[25] D. Ivanischev,[49] Y. Iwanaga,[20] B. V. Jacak,[57,†] J. Jia,[5,56] X. Jiang,[34] B. M. Johnson,[5] T. Jones,[1] K. S. Joo,[41] D. Jouan,[47] J. Kamin,[57] S. Kaneti,[57] B. H. Kang,[19] J. H. Kang,[63] J. S. Kang,[19] J. Kapustinsky,[34] K. Karatsu,[31,50] M. Kasai,[52,50] D. Kawall,[38,51] A. V. Kazantsev,[30] T. Kempel,[24] A. Khanzadeev,[49] K. M. Kijima,[20] B. I. Kim,[29] D. J. Kim,[26] E. J. Kim,[8] Y.-J. Kim,[22] Y. K. Kim,[19] E. Kinney,[11] Á. Kiss,[15] E. Kistenev,[5] D. Kleinjan,[6] P. Kline,[57] L. Kochenda,[49] B. Komkov,[49] M. Konno,[60] J. Koster,[22] D. Kotov,[49] A. Král,[13] G. J. Kunde,[34] K. Kurita,[52,50] M. Kurosawa,[50] Y. Kwon,[63] G. S. Kyle,[44] R. Lacey,[56] Y. S. Lai,[12] J. G. Lajoie,[24] A. Lebedev,[24] D. M. Lee,[34] J. Lee,[16] K. B. Lee,[29] K. S. Lee,[29] S. H. Lee,[57] S. R. Lee,[8] M. J. Leitch,[34] M. A. L. Leite,[54] P. Lichtenwalner,[40] S. H. Lim,[63] L. A. Linden Levy,[11] A. Litvinenko,[25] H. Liu,[34] M. X. Liu,[34] X. Li,[9] B. Love,[61] D. Lynch,[5] C. F. Maguire,[61] Y. I. Makdisi,[4] A. Malakhov,[25] A. Manion,[57] V. I. Manko,[30] E. Mannel,[12] Y. Mao,[48,50] H. Masui,[60] M. McCumber,[57] P. L. McGaughey,[34] D. McGlinchey,[17] C. McKinney,[22] N. Means,[57] M. Mendoza,[6] B. Meredith,[22] Y. Miake,[60] T. Mibe,[27] A. C. Mignerey,[37] K. Miki,[60] A. Milov,[62] J. T. Mitchell,[5] Y. Miyachi,[50,59] A. K. Mohanty,[3] H. J. Moon,[41] Y. Morino,[10] A. Morreale,[6] D. P. Morrison,[5] S. Motschwiller,[40] T. V. Moukhanova,[30] T. Murakami,[31] J. Murata,[52,50] S. Nagamiya,[27] J. L. Nagle,[11] M. Naglis,[62] M. I. Nagy,[28] I. Nakagawa,[50,51] Y. Nakamiya,[20] K. R. Nakamura,[31,50] T. Nakamura,[50] K. Nakano,[50] J. Newby,[33] M. Nguyen,[57] M. Nihashi,[20] R. Nouicer,[5] A. S. Nyanin,[30] C. Oakley,[18] E. O'Brien,[5] C. A. Ogilvie,[24] K. Okada,[51] M. Oka,[60] A. Oskarsson,[36] M. Ouchida,[20] K. Ozawa,[10] R. Pak,[5] V. Pantuev,[57] V. Papavassiliou,[44] B. H. Park,[19] I. H. Park,[16] S. K. Park,[29] S. F. Pate,[44] H. Pei,[24] J.-C. Peng,[22] H. Pereira,[14] V. Peresedov,[25] D. Yu. Peressounko,[30] R. Petti,[57] C. Pinkenburg,[5] R. P. Pisani,[5] M. Proissl,[57] M. L. Purschke,[5] H. Qu,[18] J. Rak,[26] I. Ravinovich,[62] K. F. Read,[46,58] K. Reygers,[39] V. Riabov,[49] Y. Riabov,[49] E. Richardson,[37] D. Roach,[61] G. Roche,[35] S. D. Rolnick,[6] M. Rosati,[24] S. S. E. Rosendahl,[36] P. Rukoyatkin,[25] B. Sahlmueller,[39] N. Saito,[27] T. Sakaguchi,[5] V. Samsonov,[49] S. Sano,[10] M. Sarsour,[18] T. Sato,[60] M. Savastio,[57] S. Sawada,[27] K. Sedgwick,[6] R. Seidl,[51] R. Seto,[6] D. Sharma,[62] I. Shein,[21] T.-A. Shibata,[50,59] K. Shigaki,[20] H. H. Shim,[29] M. Shimomura,[60] K. Shoji,[31,50] P. Shukla,[3] A. Sickles,[5] C. L. Silva,[24] D. Silvermyr,[46] C. Silvestre,[14] K. S. Sim,[29] B. K. Singh,[2] C. P. Singh,[2] V. Singh,[2] M. Slunečka,[7] T. Sodre,[40] R. A. Soltz,[33] W. E. Sondheim,[34] S. P. Sorensen,[58] I. V. Sourikova,[5] P. W. Stankus,[46] E. Stenlund,[36] S. P. Stoll,[5] T. Sugitate,[20] A. Sukhanov,[5] J. Sun,[57] J. Sziklai,[28] E. M. Takagui,[54] A. Takahara,[10] A. Taketani,[50,51] R. Tanabe,[60] Y. Tanaka,[42] S. Taneja,[57] K. Tanida,[31,50,51,55] M. J. Tannenbaum,[5] S. Tarafdar,[2] A. Taranenko,[56] E. Tennant,[44] H. Themann,[57] D. Thomas,[1] M. Togawa,[51] L. Tomášek,[23] M. Tomášek,[23] H. Torii,[20] R. S. Towell,[1] I. Tserruya,[62] Y. Tsuchimoto,[20] K. Utsunomiya,[10] C. Vale,[5] H. W. van Hecke,[34] E. Vazquez-Zambrano,[12] A. Veicht,[12] J. Velkovska,[61] R. Vértesi,[28] M. Virius,[13] A. Vossen,[22] V. Vrba,[23] E. Vznuzdaev,[49] X. R. Wang,[44] D. Watanabe,[20] K. Watanabe,[60] Y. Watanabe,[50,51] Y. S. Watanabe,[10] F. Wei,[24] R. Wei,[56] J. Wessels,[39] S. N. White,[5] D. Winter,[12] C. L. Woody,[5] R. M. Wright,[1] M. Wysocki,[11] Y. L. Yamaguchi,[10] R. Yang,[22]

A. Yanovich,[21] J. Ying,[18] S. Yokkaichi,[50,51] J. S. Yoo,[16] G. R. Young,[46] I. Younus,[43] Z. You,[34,48] I. E. Yushmanov,[30] W. A. Zajc,[12] A. Zelenski,[4] S. Zhou,[9] and L. Zolin[25]

(PHENIX Collaboration)

[1]*Abilene Christian University, Abilene, Texas 79699, USA*
[2]*Department of Physics, Banaras Hindu University, Varanasi 221005, India*
[3]*Bhabha Atomic Research Centre, Bombay 400085, India*
[4]*Collider-Accelerator Department, Brookhaven National Laboratory, Upton, New York 11973-5000, USA*
[5]*Physics Department, Brookhaven National Laboratory, Upton, New York 11973-5000, USA*
[6]*University of California - Riverside, Riverside, California 92521, USA*
[7]*Charles University, Ovocný trh 5, Praha 1, 116 36, Prague, Czech Republic*
[8]*Chonbuk National University, Jeonju, 561-756, Korea*
[9]*China Institute of Atomic Energy (CIAE), Beijing, People's Republic of China*
[10]*Center for Nuclear Study, Graduate School of Science, University of Tokyo, 7-3-1 Hongo, Bunkyo, Tokyo 113-0033, Japan*
[11]*University of Colorado, Boulder, Colorado 80309, USA*
[12]*Columbia University, New York, New York 10027 and Nevis Laboratories, Irvington, New York 10533, USA*
[13]*Czech Technical University, Zikova 4, 166 36 Prague 6, Czech Republic*
[14]*Dapnia, CEA Saclay, F-91191, Gif-sur-Yvette, France*
[15]*ELTE, Eötvös Loránd University, H - 1117 Budapest, Pázmány P. s. 1/A, Hungary*
[16]*Ewha Womans University, Seoul 120-750, Korea*
[17]*Florida State University, Tallahassee, Florida 32306, USA*
[18]*Georgia State University, Atlanta, Georgia 30303, USA*
[19]*Hanyang University, Seoul 133-792, Korea*
[20]*Hiroshima University, Kagamiyama, Higashi-Hiroshima 739-8526, Japan*
[21]*IHEP Protvino, State Research Center of Russian Federation, Institute for High Energy Physics, Protvino, 142281, Russia*
[22]*University of Illinois at Urbana-Champaign, Urbana, Illinois 61801, USA*
[23]*Institute of Physics, Academy of Sciences of the Czech Republic, Na Slovance 2, 182 21 Prague 8, Czech Republic*
[24]*Iowa State University, Ames, Iowa 50011, USA*
[25]*Joint Institute for Nuclear Research, 141980 Dubna, Moscow Region, Russia*
[26]*Helsinki Institute of Physics and University of Jyväskylä, P.O. Box 35, FI-40014 Jyväskylä, Finland*
[27]*KEK, High Energy Accelerator Research Organization, Tsukuba, Ibaraki 305-0801, Japan*
[28]*KFKI Research Institute for Particle and Nuclear Physics of the Hungarian Academy of Sciences (MTA KFKI RMKI), H-1525 Budapest 114, P.O. Box 49, Budapest, Hungary*
[29]*Korea University, Seoul, 136-701, Korea*
[30]*Russian Research Center "Kurchatov Institute", Moscow, Russia*
[31]*Kyoto University, Kyoto 606-8502, Japan*
[32]*Laboratoire Leprince-Ringuet, Ecole Polytechnique, CNRS-IN2P3, Route de Saclay, F-91128, Palaiseau, France*
[33]*Lawrence Livermore National Laboratory, Livermore, California 94550, USA*
[34]*Los Alamos National Laboratory, Los Alamos, New Mexico 87545, USA*
[35]*LPC, Université Blaise Pascal, CNRS-IN2P3, Clermont-Fd, 63177 Aubiere Cedex, France*
[36]*Department of Physics, Lund University, Box 118, SE-221 00 Lund, Sweden*
[37]*University of Maryland, College Park, Maryland 20742, USA*
[38]*Department of Physics, University of Massachusetts, Amherst, Massachusetts 01003-9337, USA*
[39]*Institut fur Kernphysik, University of Muenster, D-48149 Muenster, Germany*
[40]*Muhlenberg College, Allentown, Pennsylvania 18104-5586, USA*
[41]*Myongji University, Yongin, Kyonggido 449-728, Korea*
[42]*Nagasaki Institute of Applied Science, Nagasaki-shi, Nagasaki 851-0193, Japan*
[43]*University of New Mexico, Albuquerque, New Mexico 87131, USA*
[44]*New Mexico State University, Las Cruces, New Mexico 88003, USA*
[45]*Department of Physics and Astronomy, Ohio University, Athens, Ohio 45701, USA*
[46]*Oak Ridge National Laboratory, Oak Ridge, Tennessee 37831, USA*
[47]*IPN-Orsay, Universite Paris Sud, CNRS-IN2P3, BP1, F-91406, Orsay, France*
[48]*Peking University, Beijing, People's Republic of China*
[49]*PNPI, Petersburg Nuclear Physics Institute, Gatchina, Leningrad region, 188300, Russia*
[50]*RIKEN Nishina Center for Accelerator-Based Science, Wako, Saitama 351-0198, Japan*
[51]*RIKEN BNL Research Center, Brookhaven National Laboratory, Upton, New York 11973-5000, USA*
[52]*Physics Department, Rikkyo University, 3-34-1 Nishi-Ikebukuro, Toshima, Tokyo 171-8501, Japan*
[53]*Saint Petersburg State Polytechnic University, St. Petersburg, Russia*
[54]*Universidade de São Paulo, Instituto de Física, Caixa Postal 66318, São Paulo CEP05315-970, Brazil*

[55]Seoul National University, Seoul, Korea
[56]Chemistry Department, Stony Brook University, SUNY, Stony Brook, New York 11794-3400, USA
[57]Department of Physics and Astronomy, Stony Brook University, SUNY, Stony Brook, New York 11794-3400, USA
[58]University of Tennessee, Knoxville, Tennessee 37996, USA
[59]Department of Physics, Tokyo Institute of Technology, Oh-okayama, Meguro, Tokyo 152-8551, Japan
[60]Institute of Physics, University of Tsukuba, Tsukuba, Ibaraki 305, Japan
[61]Vanderbilt University, Nashville, Tennessee 37235, USA
[62]Weizmann Institute, Rehovot 76100, Israel
[63]Yonsei University, IPAP, Seoul 120-749, Korea
(Received 3 September 2010; published 11 February 2011)

Large parity-violating longitudinal single-spin asymmetries $A_L^{e^+} = -0.86^{+0.30}_{-0.14}$ and $A_L^{e^-} = 0.88^{+0.12}_{-0.71}$ are observed for inclusive high transverse momentum electrons and positrons in polarized $p + p$ collisions at a center-of-mass energy of $\sqrt{s} = 500$ GeV with the PHENIX detector at RHIC. These $e^{\pm}$ come mainly from the decay of $W^{\pm}$ and Z^0 bosons, and their asymmetries directly demonstrate parity violation in the couplings of the $W^{\pm}$ to the light quarks. The observed electron and positron yields were used to estimate $W^{\pm}$ boson production cross sections for the $e^{\pm}$ channels of $\sigma(pp \to W^+X) \times \mathrm{BR}(W^+ \to e^+\nu_e) = 144.1 \pm 21.2(\mathrm{stat})^{+3.4}_{-10.3}(\mathrm{syst}) \pm 21.6(\mathrm{norm})$ pb, and $\sigma(pp \to W^-X) \times \mathrm{BR}(W^- \to e^-\bar{\nu}_e) = 31.7 \pm 12.1(\mathrm{stat})^{+10.1}_{-8.2}(\mathrm{syst}) \pm 4.8(\mathrm{norm})$ pb.

DOI: 10.1103/PhysRevLett.106.062001 PACS numbers: 13.88.+e, 14.20.Dh, 14.70.Fm, 25.40.Ep

Determining the contributions of the partons to the spin of the proton is a crucial element in our understanding of quantum chromodynamics (QCD) [1–3]. Polarized inclusive deep inelastic scattering (DIS) experiments have measured the combination of valence-and-sea-quark ($\Delta q + \Delta\bar{q}$) and gluon-helicity (Δg) distributions [3,4]. Analyses of polarized semi-inclusive DIS experiments [5–7] have determined the individual flavor separated Δq and $\Delta\bar{q}$ by connecting final state hadrons with quark flavors using fragmentation functions. Collisions of longitudinally polarized protons at high energies allow for the study of Δg [4,8,9] and can provide complementary measurements of up (Δu, $\Delta\bar{u}$) and down (Δd, $\Delta\bar{d}$) quarks [10,11]. In particular, W bosons couple only the left-handed quarks and right-handed antiquarks ($u_L\bar{d}_R \to W^+$ and $d_L\bar{u}_R \to W^-$), so the asymmetry of the W yield from flipping the helicity of a polarized proton is sensitive to the flavor dependence of Δq and $\Delta\bar{q}$. Production of the W occurs at a scale where higher order QCD corrections can be evaluated reliably, and it is free from uncertainties in fragmentation functions by detecting leptons from W decay [12,13]. The measured W cross sections in spin-averaged collisions at $\sqrt{s} = 500$ GeV confirm theoretical understanding of the production processes.

The first observations of W-boson production in polarized $p + p$ collisions, and direct demonstration of the parity-violating coupling of the W to the light quarks are reported here by PHENIX and in a companion paper by STAR [14] for $\sqrt{s} = 500$ GeV at the Relativistic Heavy Ion Collider (RHIC). The 2009 PHENIX data are from polarized $pp \to e^{\pm} + X$, where the $e^{\pm}$ with transverse momentum $p_T > 30$ GeV/c come mainly from W and Z decays.

The PHENIX detector has been described in detail elsewhere [15]. This analysis uses data from the two central arm spectrometers, each covering $|\Delta\phi| < \pi/2$ in azimuth and $|\eta| < 0.35$ in pseudorapidity. Charged track momenta are determined by measuring their bend angle in an axial magnetic field using drift chambers outside the field starting at a radius of 2.02 m from the beamline. The longitudinal position, z, of each track is determined by pad chambers at 2.46 m, with spatial resolution of $\sigma_z = 1.7$ mm. The electromagnetic calorimeter, located at a radial distance of $\sim$5 m from the beam line, determines the energy, position, and time of flight of electrons. In this analysis, the p_T dependence of the reconstructed π^0 and η mass peaks was used to confirm the energy scale and linearity to within 2.5%. The p_T dependence of the peak widths indicates an energy resolution $\sigma_E/E = 8.1\%/\sqrt{E(\mathrm{GeV})} \oplus 5.0\%$.

A trigger with a nominal 10 GeV threshold in the electromagnetic calorimeter selected events for this analysis. This trigger was fully efficient for $e^{\pm}$ with p_T above 12 GeV/c. Charged tracks in the drift and pad chambers matching calorimeter clusters with $|\Delta\phi| < 0.01$ were used to reconstruct the z position of the event vertex. Only events with $|z| < 30$ cm were used. Loose cuts on the time of flight measured by the calorimeter and energy-momentum matching suppressed accidental matches and cosmic rays.

The analyzed data sample corresponds to an integrated luminosity of 8.6 pb^{-1}, which was determined from beam-beam counter coincidences and corrected for a small (6%) effect from multiple collisions per beam crossing. The beam-beam counters are two arrays of 64 quartz Čerenkov counters located at $3.1 < |\eta| < 3.9$. The cross section for coincidences within $|z| \lesssim 30$ cm was found to be 32.5 ± 3.2 mb from the van der Meer scan technique [16].

The resulting yield of positive and negative electron candidates is shown in Fig. 1 where p_T has been determined

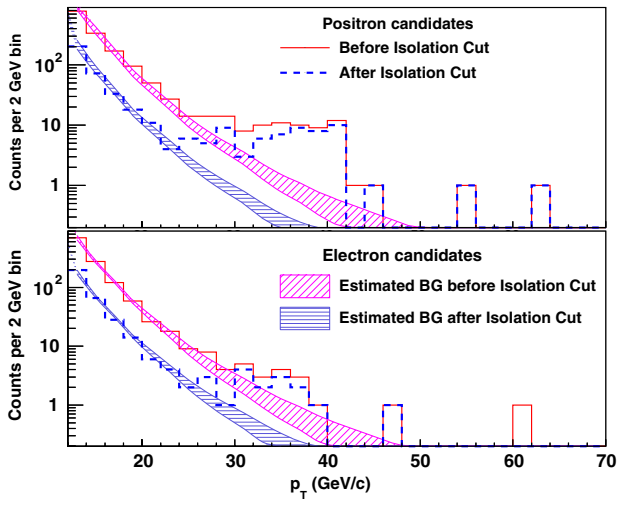

FIG. 1 (color online). The spectra of positron (upper panel) and electron (lower panel) candidates before (solid histogram) and after (dashed histogram) an isolation cut. The bands reflect the uncertainty of the background.

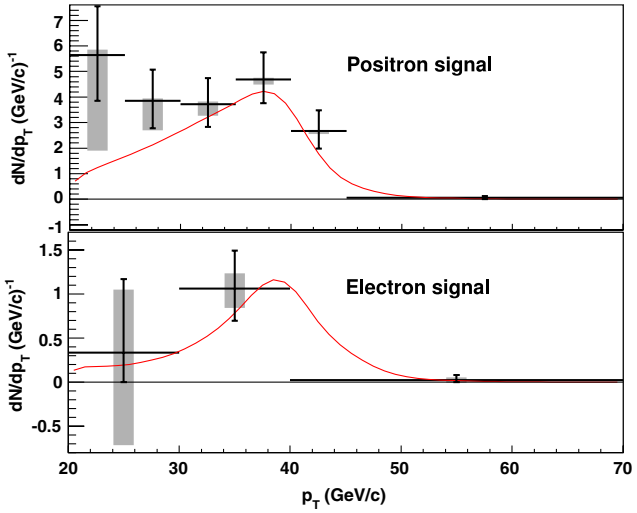

FIG. 2 (color online). Background subtracted spectra of positron (upper panel) and electron (lower panel) candidates before the isolation cut compared to the spectrum of W and Z decays from an NLO calculation [12,13]. The gray bands reflect the uncertainty of the background.

from the calorimeter cluster energy. The charge sign is determined from the bend angle, α, measured in the drift chamber, and the nominal transverse beam position. The angular resolution and stability of beam position were monitored by frequent runs with no magnetic field. The resolution σ_α was typically about 1.1 mr, to be compared to a 2.3 mr bend angle for 40 GeV/c tracks. The variation in the average transverse beam position measured by reconstruction of the primary vertex in these runs was within ± 300 μm, and did not affect the charge determination. The probability of charge misidentification at 40 GeV/c was estimated to be less than 2%.

In addition to $e^{\pm}$ from W and Z decay, this sample of events contains various backgrounds. The dominant backgrounds were photon conversions before the drift chamber and charged hadrons. These were estimated using the raw calorimeter cluster distribution and the charged pion spectra predicted by perturbative QCD convoluted with the hadronic response of the calorimeter tuned to reproduce test beam data. This calculated background was normalized to the measured spectrum in the region $12 < p_T < 20$ GeV/c and extrapolated to higher p_T. Electrons from heavy flavor decay were estimated from a fixed-order-next-to-leading-logarithm calculation [17], which agrees well with the prompt electron measurement at $\sqrt{s} = 200$ GeV [18]. PYTHIA [19] was used to estimate the contributions of electrons with $p_T > 30$ GeV/c from sequential τ lepton decays of W and Z bosons. These two components were found to be negligible. The background bands in Fig. 1 include uncertainties in the photon conversion probability, the background normalization, and the background extrapolation to $p_T > 30$ GeV/c.

The tracks within the nominal geometric acceptance of the central spectrometer were reconstructed with ~37% efficiency defined by the overlap of live areas in the tracking detectors, and fiducial areas on the calorimeters and drift chambers. The efficiency for retaining electron candidates after all cuts was 99%. The resulting reconstruction efficiency was not p_T dependent for $p_T > 30$ GeV/c.

Figure 2 shows the background subtracted signal for positive and negative charges compared to the next-to-leading-order (NLO) [12,13] calculated spectrum, which is normalized for the integrated luminosity, corrected for the detector efficiency and acceptance, and smeared by the energy resolution of the calorimeter. The cross sections measured by counting events in the signal region ($30 < p_T < 50$ GeV/c) are consistent with the NLO and next-to-NLO (NNLO) [20] calculations shown in Table I. The systematic uncertainties in the measurement include the uncertainty in the background and a 15% normalization uncertainty due to the luminosity (10%), multiple collision

TABLE I. Comparison of measured cross sections for electrons and positrons with $30 < p_T < 50$ GeV/c from W and Z decays with NLO [12,13] and NNLO [20] calculations. The first error is statistical, the second error is systematic from the uncertainty in the background, and the third error is a normalization uncertainty.

	$\frac{d\sigma}{dy}(30 < p_T^e < 50\ \text{GeV}/c)\|_{y=0}$ [pb]		
Lepton	Data	NLO	NNLO
e^+	$50.2 \pm 7.2^{+1.2}_{-3.6} \pm 7.5$	43.2	46.8
e^-	$9.7 \pm 3.7^{+2.1}_{-2.5} \pm 1.5$	11.3	13.5
e^+ and e^-	$59.9 \pm 8.1^{+3.1}_{-6.0} \pm 9.0$	54.5	60.3

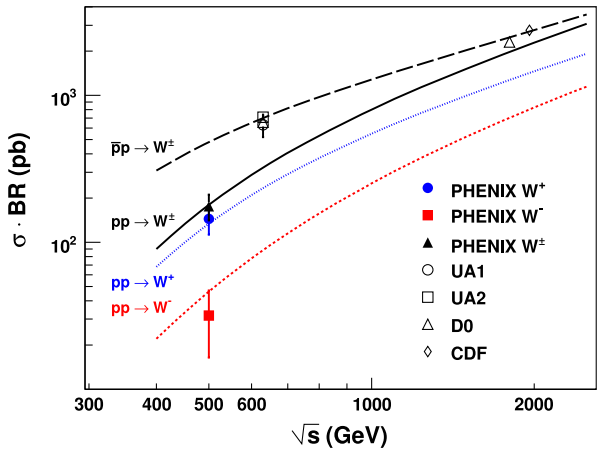

FIG. 3 (color online). Inclusive cross sections for W leptonic decay channel of this measurement and $\bar{p}p$ measurements [23–26]. Statistical and systematic uncertainties were added here in quadrature. The curves are theory calculations [20].

(5%), and acceptance and efficiency uncertainties (10%). To compute the $W^{\pm}$ production cross sections, we used the NLO and NNLO calculations to subtract the Z contribution in our sample and to correct for W decays that were outside of the detector acceptance. The contribution from Z decays is 6.9% for W^+ and 30.6% for W^-. The fraction of the total cross section within $|y| < 0.35$ in rapidity, $p_T > 30$ GeV/c, and $|\Delta\phi| < \pi$ is estimated to be 11.3% of positrons from W^+ and 7.4% of electrons from W^-. The theoretical uncertainties from NLO and NNLO calculations and varied parton-distribution functions (PDFs) [21,22] are small compared to other sources of systematic uncertainty. With these corrections, $\sigma(pp \to W^+X) \times \mathrm{BR}(W^+ \to e^+\nu_e) = 144.1 \pm 21.2(\mathrm{stat})^{+3.4}_{-10.3} \times (\mathrm{syst}) \pm 21.6(\mathrm{norm})$ pb, and $\sigma(pp \to W^-X) \times \mathrm{BR}(W^- \to e^-\bar{\nu}_e) = 31.7 \pm 12.1(\mathrm{stat})^{+10.1}_{-8.2} \times (\mathrm{syst}) \pm 4.8(\mathrm{norm})$ pb, where BR is the branching ratio. These are shown in Fig. 3 and compared to published Tevatron and $Sp\bar{p}S$ data [23–26].

In order to determine the longitudinal spin asymmetry with a sample of W decays with minimal background contamination, two additional requirements were imposed on the candidate events. The first cut is to reject tracks with a bend angle $|\alpha| < 1$ mr, which reduces charge misidentification to negligible levels. The second, an isolation cut to remove jets, requires the sum of cluster energies in the calorimeter and transverse momenta measured in the drift chamber to be less than 2 GeV in a cone with a radius in η and ϕ of 0.5 around the candidate track. Figure 1 shows that about 80% of the signal is kept, while the background is reduced by a factor ~4. The region $12 < p_T < 20$ GeV/c was used to extrapolate the background scaling factor, which includes the uncertainty from a possible p_T dependence and is shown as the lower band. After these two additional cuts, there are 42 candidate $W^+ + Z^0$ decays to positrons with a background of 1.7 ± 1.0 and 13 candidate $W^- + Z^0$ decays to electrons with a background of 1.6 ± 1.0 events within $30 < p_T < 50$ GeV/c.

The measured asymmetry is given by

$$\epsilon_L = \frac{N^+ - RN^-}{N^+ + RN^-} \tag{1}$$

where N^+ is the number of events from a beam of positive helicity and N^- is the number of events from a beam of negative helicity, and R is the ratio of the luminosity for the positive and the negative helicity beams. The longitudinal spin asymmetry is then calculated from the measured asymmetry according to

$$A_L = \frac{\epsilon_L D}{P}, \tag{2}$$

where P is the beam polarization and D is a dilution correction to account for the remaining background in the signal region.

The two RHIC beams, with luminosity-weighted average polarizations of 0.38 ± 0.03 and 0.40 ± 0.04, provide independent measurements of A_L. The longitudinal polarization fractions were monitored using very forward neutron asymmetries [27] and found to be 99% or greater. The contribution to A_L from the small transverse component of the polarization was negligible. In RHIC, both beams are bunched, and the bunch helicity alternates almost every crossing to reduce systematic effects. The relative luminosities of different helicity combinations were measured by the beam-beam counters, and were all within 1% of each other. To treat the low statistics data properly, a likelihood function created from the four spin sorted yields corresponding to the two polarized beams was used to determine the single-spin asymmetry within its physical range $[-1, 1]$.

The measured asymmetries are shown in Table II for tracks in the background $(12 < p_T < 20$ GeV/$c)$ and signal $(30 < p_T < 50$ GeV/$c)$ regions. For tracks in the background region, ϵ_L was found to be zero within

TABLE II. Longitudinal single-spin asymmetries. The confidence intervals are defined for A_L^e.

Sample	ϵ_L	$A_L^e(W+Z)$	68% C.L.	95% C.L.
Background +	-0.015 ± 0.04			
Signal +	-0.31 ± 0.10	-0.86	$[-1, -0.56]$	$[-1, -0.16]$
Background −	-0.025 ± 0.04			
Signal −	0.29 ± 0.20	$+0.88$	[0.17, 1]	$[-0.60, 1]$

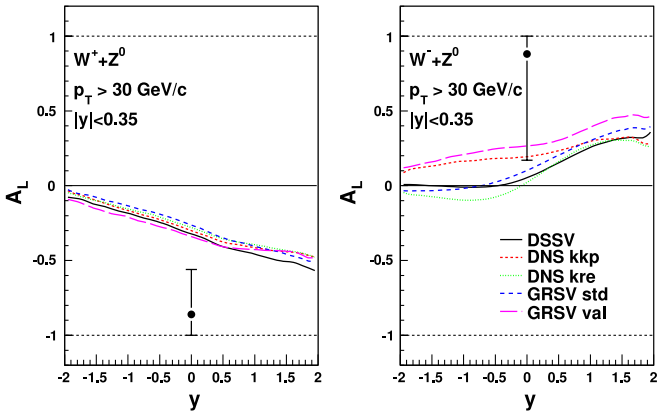

FIG. 4 (color online). Longitudinal single-spin asymmetries for electrons and positrons from W and Z decays. The error bars represent 68% C.L. The theoretical curves are calculated using NLO with different polarized PDFs [12].

uncertainties. A significant nonzero asymmetry was observed for positrons in the signal region. The dilution corrections of $D = 1.04 \pm 0.03$ and 1.14 ± 0.10 for positive and negative charges, respectively, were applied to account for the parity-conserving background.

Figure 4 compares measured longitudinal single-spin asymmetries to estimates based on a sample of polarized PDFs extracted from fits of DIS and semi-inclusive DIS data [12]. The experimental results are consistent with the theoretical calculations at 6%–15% confidence level for $A_L^{e^+}$ and at 20%–37% for $A_L^{e^-}$. The observed asymmetries are sensitive to the polarized quark densities at $x \sim M_W/\sqrt{s} \simeq 0.16$, and directly demonstrate the parity-violating coupling between W bosons and light quarks.

In summary, we present first measurements of production cross section and nonzero parity-violating asymmetry in W and Z production in polarized $p + p$ collisions at $\sqrt{s} = 500$ GeV. The results are found to be consistent with theoretical expectations and similar measurements of $A_L^{e^\pm}$ [14]. RHIC luminosity and PHENIX detector upgrades in progress will make it possible in the future to significantly reduce the uncertainties for A_L and to extend the measurement to forward rapidity, which will improve our knowledge of flavor-separated quark and antiquark helicity distributions.

We thank the Collider-Accelerator Department for developing the unique technologies enabling these measurements and the Physics Department staff at BNL for vital contributions. We also thank D. de Florian, B. Surrow, and J. Balewski for helpful discussions. We acknowledge support from the Office of Nuclear Physics in DOE Office of Science and NSF (USA), MEXT and JSPS (Japan), CNPq and FAPESP (Brazil), NSFC (China), MSMT (Czech Republic), IN2P3/CNRS and CEA (France), BMBF, DAAD, and AvH (Germany), OTKA (Hungary), DAE and DST (India), ISF (Israel), NRF and WCU (Korea), MES, RAS, and FAAE (Russia), VR and KAW (Sweden), U.S. CRDF for the FSU, Hungary-U.S. HAESF, and U.S.-Israel BSF.

*Deceased
†Spokesperson: jacak@skipper.physics.sunysb.edu

[1] R. L. Jaffe and A. Manohar, Nucl. Phys. **B337**, 509 (1990).
[2] E. Leader and M. Anselmino, Z. Phys. C **41**, 239 (1988).
[3] S. E. Kuhn, J. P. Chen, and E. Leader, Prog. Part. Nucl. Phys. **63**, 1 (2009), and references therein.
[4] D. de Florian, R. Sassot, M. Stratmann, and W. Vogelsang, Phys. Rev. D **80**, 034030 (2009).
[5] M. G. Alekseev *et al.*, Phys. Lett. B **693**, 227 (2010).
[6] A. Airapetian *et al.*, Phys. Rev. D **71**, 012003 (2005).
[7] B. Adeva *et al.*, Phys. Lett. B **420**, 180 (1998).
[8] A. Adare *et al.*, Phys. Rev. Lett. **103**, 012003 (2009).
[9] B. I. Abelev *et al.*, Phys. Rev. Lett. **100**, 232003 (2008).
[10] G. Bunce, N. Saito, J. Soffer, and W. Vogelsang, Annu. Rev. Nucl. Part. Sci. **50**, 525 (2000).
[11] C. Bourrely and J. Soffer, Phys. Lett. B **314**, 132 (1993).
[12] D. de Florian and W. Vogelsang, Phys. Rev. D **81**, 094020 (2010).
[13] P. M. Nadolsky and C. P. Yuan, Nucl. Phys. **B666**, 31 (2003).
[14] M. M. Aggarwal *et al.*, Phys. Rev. Lett. **106**, 062002 (2011).
[15] K. Adcox *et al.*, Nucl. Instrum. Methods Phys. Res., Sect. A **499**, 469 (2003).
[16] A. Adare *et al.*, Phys. Rev. D **79**, 012003 (2009).
[17] M. Cacciari, P. Nason, and R. Vogt, Phys. Rev. Lett. **95**, 122001 (2005); M. Cacciari (private communication).
[18] A. Adare *et al.*, Phys. Rev. Lett. **97**, 252002 (2006).
[19] T. Sjöstrand *et al.*, Comput. Phys. Commun. **135**, 238 (2001).
[20] K. Melnikov and F. Petriello, Phys. Rev. D **74**, 114017 (2006).
[21] A. D. Martin, R. G. Roberts, W. J. Stirling, and R. S. Thorne, Eur. Phys. J. C **28**, 455 (2003).
[22] A. D. Martin, W. J. Stirling, R. S. Thorne, and G. Watt, Eur. Phys. J. C **63**, 189 (2009).
[23] D. E. Acosta *et al.*, Phys. Rev. Lett. **94**, 091803 (2005).
[24] B. Abbott *et al.*, Phys. Rev. D **61**, 072001 (2000).
[25] J. Alitti *et al.*, Z. Phys. C **47**, 11 (1990).
[26] C. Albajar *et al.*, Z. Phys. C **44**, 15 (1989).
[27] A. Adare *et al.*, Phys. Rev. D **76**, 051106 (2007).